

Soft Matter

Accepted Manuscript



This is an *Accepted Manuscript*, which has been through the Royal Society of Chemistry peer review process and has been accepted for publication.

Accepted Manuscripts are published online shortly after acceptance, before technical editing, formatting and proof reading. Using this free service, authors can make their results available to the community, in citable form, before we publish the edited article. We will replace this *Accepted Manuscript* with the edited and formatted *Advance Article* as soon as it is available.

You can find more information about *Accepted Manuscripts* in the [Information for Authors](#).

Please note that technical editing may introduce minor changes to the text and/or graphics, which may alter content. The journal's standard [Terms & Conditions](#) and the [Ethical guidelines](#) still apply. In no event shall the Royal Society of Chemistry be held responsible for any errors or omissions in this *Accepted Manuscript* or any consequences arising from the use of any information it contains.

1 **Porosity of silica Stöber particles determined by spin-echo small**
2 **angle neutron scattering**

3 S.R.Parnell,^{1,2} A.L.Washington,^{3,4} A.J.Parnell,³ A.Walsh,⁵ R.M.Dalglish,⁶
4 F.Li,² W.A.Hamilton,⁷ S.Prevoost,⁸ J.P.A.Fairclough,⁴ and R.Pynn^{2,7}

5 ¹*Faculty of Applied Sciences, Delft University of Technology,*
6 *Mekelweg 15, 2629 JB Delft, The Netherlands*

7 ²*Centre for Exploration of Energy and Matter,*
8 *Indiana University, Bloomington, USA, 47408*

9 ³*Department of Physics and Astronomy,*
10 *The University of Sheffield, Sheffield, UK, S3 7RH*

11 ⁴*Department of Mechanical Engineering,*
12 *The University of Sheffield, Sheffield, UK, S1 3DJ*

13 ⁵*Department of Chemistry, The University of Sheffield, Sheffield, UK, S3 7HF*

14 ⁶*ISIS, Rutherford Appleton Laboratory,*
15 *Chilton, Oxfordshire, UK, OX11 0QX*

16 ⁷*Neutron Sciences Directorate, Oak Ridge National Laboratory, Oak Ridge, USA, 37831*

17 ⁸*ID02 Beamline, European Synchrotron Radiation Facility, F38043, Grenoble, France*

18 (Dated: March 11, 2016)

Abstract

Stöber silica particles are used in a diverse range of applications. Despite their widespread industrial and scientific uses, information on the internal structure of the particles is non-trivial to obtain and is not often reported. In this work we have used spin-echo small angle neutron scattering (SESANS) in conjunction with ultra small angle x-ray scattering (USAXS) and pycnometry to study an aqueous dispersion of Stöber particles. Our results are in agreement with models which propose that Stöber particles have a porous core, with a significant fraction of the pores inaccessible to solvent.

For samples prepared from the same master sample in a range of H₂O : D₂O ratio solutions we were able to model the SESANS results for the solution series assuming monodisperse, smooth surfaced spheres of radius 83 nm with an internal open pore volume fraction of 32% and a closed pore fraction of 10%. Our results are consistent with USAXS measurements. The protocol developed and discussed here shows that the SESANS technique is a powerful way to investigate particles much larger than those studied using conventional small angle scattering methods.

19 INTRODUCTION

20 Silica particles have applications in a diverse range of industrial and technological appli-
21 cations. Examples include information and communications technologies, medicine, biology
22 and environmental monitoring [1–3]. Since these applications often require control over the
23 particle size and density, significant efforts have been applied to the accurate determina-
24 tion of these parameters [4]. Conventional size determination methods such as nanoparticle
25 tracking analysis, transmission electron microscopy (TEM) and dynamic light scattering
26 (DLS) are often used.

27 One of the most common and important methods of forming silica particles uses the
28 process developed by Stöber and co workers in the 1960's [5], which is known to give superior
29 control over the particle size dispersity- an advantage reflected in over 8000 citations (to date)
30 on the original paper outlining the method. The excellent uniformity which makes Stöber
31 particles so useful also makes them suitable for more detailed structural characterisation and
32 a number of scattering experiments have been performed on these particles - the regularity
33 of the process even allowing Small Angle X-ray Scattering (SAXS) and Ultra Small Angle
34 X-ray Scattering (USAXS) measurements to be made during particle formation. These
35 showed that the particles initially nucleate as a ramified fractal structure which then grow
36 by aggregating silica from solution [6, 7] while becoming more compact as the reaction
37 proceeds. Similar results were found more recently by Pontoni et al. [8] showing nucleation
38 from a single small particle to a size of $\approx 20\text{nm}$. Once fully formed the particles have
39 been studied in greater depth [4, 9–11]. Proposed particle structures have been presented
40 by several groups with larger silica particles formed by this aggregation and clumping of
41 much smaller particles - with radii of the order 14nm [12]. In smaller Stöber particles (a
42 few tens of nm) however, no core-shell structure is observed, rather a heterogeneous open
43 structure is observed [13]. In most cases the polydispersity of Stöber particles is seen to
44 decrease with increasing reaction time and in microscopy studies this has been associated
45 with development of a pronounced smooth particle surface (see for example [14]).

46 Whilst a significant number of studies have looked at the structure of Stöber silica, very
47 few have looked at the porosity although this would seem to be a necessary concomitant
48 of the fast nucleation and slower growth model outlined above. In one study [9] helium
49 pycnometry was used to measure the Stöber silica densities, finding values initially in the

50 range of 2.04-2.10 g/cm³ for particles in the 80-900 nm size range, approximately a density
51 80% of that of crystalline quartz (2.65 g/cm³). However, after rigorous washing and drying
52 at 90°C the measured density decreased to 1.9-1.95 g/cm³. It has been postulated that
53 pycnometry measurements do not measure the porosity of the entire silica particles as the
54 C_{18} from stearyl alcohol, which is sometimes used in the formation process, can effectively
55 block the pores to the helium probe gas [9].

56 In order to investigate the structure of colloidal Stöber particles we have applied the
57 relatively new technique of Spin-Echo Small Angle Neutron Scattering (SESANS) [15–17].
58 Briefly SESANS uses a series of magnetic fields to encode the scattering angle information
59 into the polarisation of a neutron beam, a more detailed description is presented in Appendix
60 A. The structural length scale probed depends upon the applied magnetic field strength
61 and the neutron wavelength squared. On a time of flight neutron source where a range
62 of wavelengths are used this allows a corresponding range of length scales (termed spin
63 echo length, z) to be probed simultaneously. This technique has the ability to probe both
64 the inter-particle and intra-particle structure in suspensions of solvents, by measuring the
65 transverse projection of the real-space Debye correlation function $G(z)$, rather than its
66 Fourier transform that is obtained in the more familiar technique of Small Angle Neutron
67 Scattering (SANS). At spin echo lengths much greater than the particle radius the spin echo
68 signal depends very simply upon the difference in scattering length density (SLD) between
69 the particle and solution [18] allowing this difference to be determined very accurately. In this
70 study the particles were suspended in either pure H₂O or a mixture of H₂O and D₂O allowing
71 the neutron contrast between the particle and solution to be changed in a predictable way
72 and the particle density to be inferred with similar accuracy with an absolute minimum of
73 structural assumptions or free parameters. It is also important to note that the SESANS
74 technique allows the measurement of the total scattering in absolute terms (equation 11
75 in Appendix A) and unlike other neutron techniques the structural signal is not seriously
76 affected by incoherent (non-structural) scattering.

77 The SESANS technique is capable of examining much larger length scales (up to 10's
78 of microns) than traditional SANS and is comparable in the upper range to the accessible
79 length scales probed by ultra small angle neutron scattering (USANS) [19]. The approach
80 has a major advantage over the latter technique in that it can be applied to high concen-
81 tration samples, as multiple neutron scattering effects may be taken into account exactly

82 [20] whereas USANS is a dilute solution measurement. The technique does not change the
83 geometry of the sample, the scan ranges are determined by the applied magnetic fields and
84 since the scattering is encoded in the beam polarisation rather than determined from angu-
85 lar deviations SESANS can also employ rather divergent beams, allowing efficient use of the
86 available polarised neutron flux.

87 EXPERIMENTAL METHODS

88 A sample of monodisperse silica particles was synthesised using the method reported by
89 Stöber and co-workers [5]. For the synthesis, ethanol (30.0 g), deionised water (5.0 g, 18 M Ω)
90 and ammonium hydroxide (3.0 g 28-30% NH₃) (Aldrich) was added to a round bottom flask
91 and stirred for ten minutes at room temperature followed by the rapid addition of Tetraethyl
92 orthosilicate (3.0 g 98% TEOS) (Aldrich). The solution was left to stir at 250 rpm for 24 h
93 at room temperature. Silica particles were purified by centrifugation at 3000 rpm for 1 Hr
94 3 \times into ethanol then 3 \times into deionised water, (18.2 M Ω) H₂O (ELGA Purelab Option-Q)
95 being used exclusively in the preparation. A fraction of the prepared silica was weighed then
96 dried over 24 hours to determine the mass fraction in solution. This was determined to be
97 15%.

98 A number of different techniques were used to fully characterise the Stöber silica par-
99 ticles in conjunction with our primary SESANS measurements. Dynamic Light Scattering
100 (DLS) was performed using a Zetasizer NanoZS (Malvern instruments) to give values for
101 the intensity-average and number-average hydrodynamic diameters of the silica particles.
102 Silica dispersions were analysed using disposable cuvette cells and the results were averaged
103 over three consecutive runs. Prior to measurement the silica dispersions were diluted with
104 deionised water (18 M Ω) and filtered through a 0.20 μ m filter membrane (to remove any
105 dust). An LM10 particle tracker (Nanosight) was used to measure the size of a large number
106 of single particles via tracking the individual particle tracks, which act as point scatterers
107 and move via Brownian motion. The video footage was analysed using the inbuilt particle
108 tracking analysis software, which gave a particle hydrodynamic radius of 73 nm. DLS mea-
109 surements were also used to check the polydispersity of the samples the was measured to be
110 1%, suitably mono disperse for our sample requirements here.

111 Density measurements were made using an AccuPyc 1330 helium pycnometer (Micromet-

112 rics) with a 0.1 cm^3 sample cell. Our silica particles were dried for 24 Hr in an oven at 100°
 113 C to produce a dry powder sample suitable for analysis. Once dried the samples were then
 114 dispersed into H_2O and further diluted with D_2O as detailed below to make the different
 115 solution volume fractions. The gas pycnometer measured a density of 2.32 g cm^{-3} which is
 116 only 12.5 percent lower than the value for crystalline SiO_2 (2.65 g cm^{-3}) indicating Stöber
 117 particles of good quality. SANS investigations have returned a range of density values de-
 118 pending on sample conditions and preparation and an accepted value of good colloidal silica
 119 particles is in the region of 2.26 g cm^{-3} [21]

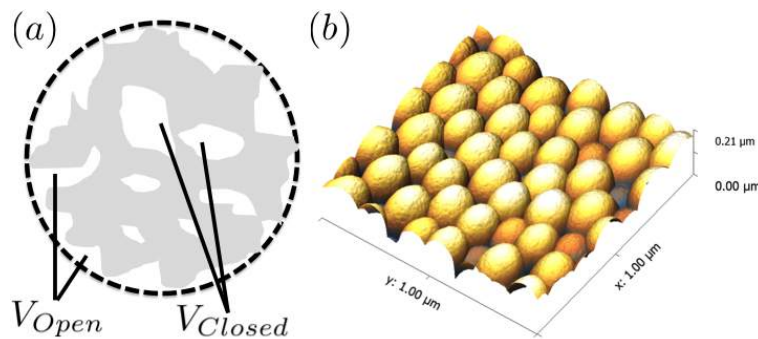


FIG. 1. (a) Schematic of porous particle, the dashed line designs the particle radius R with the volume of inaccessible voids termed V_{Closed} and the accessible voids V_{Open} and (b) AFM height image for an ensemble of spin coated SiO_2 nanoparticles.

120 The SESANS measurements were performed on the Offspec instrument [22] at the ISIS
 121 pulsed neutron and Muon source (Oxfordshire, UK). The data was normalised to the in-
 122 strumental polarisation using a blank (pure solvent) sample of the same thickness. Similar
 123 measurements were obtained on the instrument SESAME at the Low Energy Neutron Source
 124 LENS (Indiana, USA) [23, 24] and are detailed in Parnell et al. [25]. In order to conclusively
 125 check for systematic differences in the solvent scattering a series of H_2O and D_2O solvent
 126 blanks were run on the SESAME instrument in SESANS mode to check for changes in in-
 127 strumental polarisation. No changes were observed between pure D_2O and pure H_2O for
 128 blanks of 5mm path length, confirming that, as expected the incoherent background which
 129 normally arises from using H_2O in conventional neutron scattering measurements does not
 130 affect these SESANS measurements. Here the $G(z)$ for the samples was determined from a
 131 comparison of the spin echo signal with and without the sample (for details see Appendix
 132 A)

133 USAXS measurements were performed on the beamline ID02 at ESRF and SANS mea-
134 surements were performed at the LENS SANS instrument. For the dilute samples necessary
135 for USAXS measurements a sample in H₂O was diluted in concentration down to a volume
136 fraction of $\approx 1\%$. For the SANS measurements the H₂O sample was dried and redispersed
137 into D₂O to reduce incoherent scattering. The redispersed sample was sonicated for 2 hours
138 and checks were made visually to observe that the sample was fully re-dispersed.

139 RESULTS

140 A series of SESANS measurements were performed for various different combinations of
141 concentration and solvent scattering length density (SLD). They are shown in figure 2 and
142 the data were fitted using the theory presented in the appendices with the appropriate form
143 and structure factors for uniform density spheres as given in Pedersen [26]. In the process of
144 fitting the data two facts become immediately apparent. The first is that when simulating
145 the undiluted sample it has a larger radius than that determined by our DLS measurement
146 and secondly that simulations of the shape of the curves cannot model the shape of the dip
147 observed at $z=150\text{nm}$ due to the excluded volumes, which are more pronounced in the higher
148 silica concentration sample. Attempts to simulate the data to the measured mass fraction
149 (0.15) and radius (73 nm) determined from the DLS were unsuccessful. Good agreement
150 was found for a volume fraction of 0.1 rather than the 0.06 value which would be expected
151 from the measured mass fraction with the silica of the density measured by pycnometry.
152 In order to accurately simulate the asymptotic value at long spin echo length the porous
153 structure model described in the appendix was used with two additional parameters for the
154 volume fractions for the accessible and inaccessible voids in the silica particles, these are
155 V_{Open} and V_{Closed} respectively. Good agreement was found with values of $V_{Open}=0.32$ and
156 $V_{Closed}=0.10$. and the resulting fits are shown in figure 2.

157 While very accurate for measurements of overall scattering power SESANS is somewhat
158 less sensitive to small changes in particle radius compared to other techniques such as tradi-
159 tional scattering techniques and hence our best estimate of the Stöber particle radius is from
160 the dilute sample measured on ID02 at the ESRF. The measured USAXS data is shown in
161 figure 3 with a simulation to a hard sphere model with a radius of $83\pm 1\text{nm}$. This value was
162 used in the SESANS modelling, although fits of similar accuracy can be obtained for $R \approx$

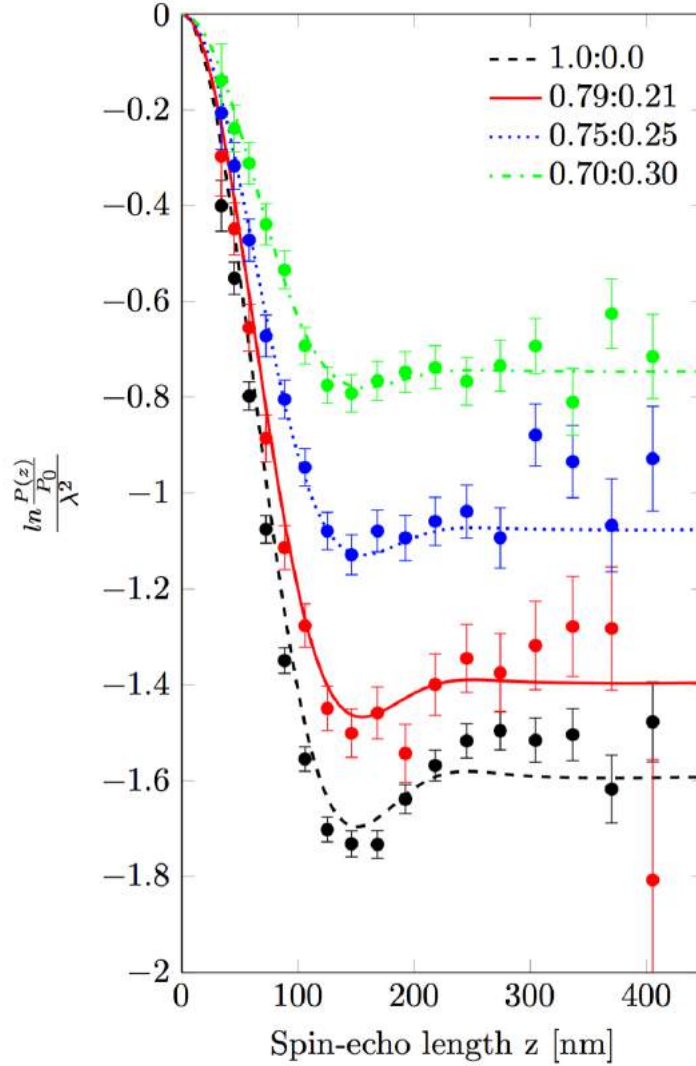


FIG. 2. The normalised spin-echo signal as a function of spin-echo length for various different dilutions of H_2O and D_2O . Note the legend indicates the ratio of H_2O to D_2O . The undiluted sample has a mass fraction of 0.15. The solid lines are calculated from the model discussed in the text.

163 $82.5 \pm 2.5 \text{ nm}$, however these do change the total porosity and porous fractions due to Σ_t
 164 being dependent on R via equations 4 and 11.

165 Finally in order to achieve information on the surface of the particles SANS was measured
 166 at LENS from a dilute (volume fraction 1.2%) sample of the same particles in D_2O . Fitting
 167 to the observed Porod surface scattering region at this higher Q is shown falling off into
 168 the incoherent background signal (4). The structural scattering intensity in this data falls

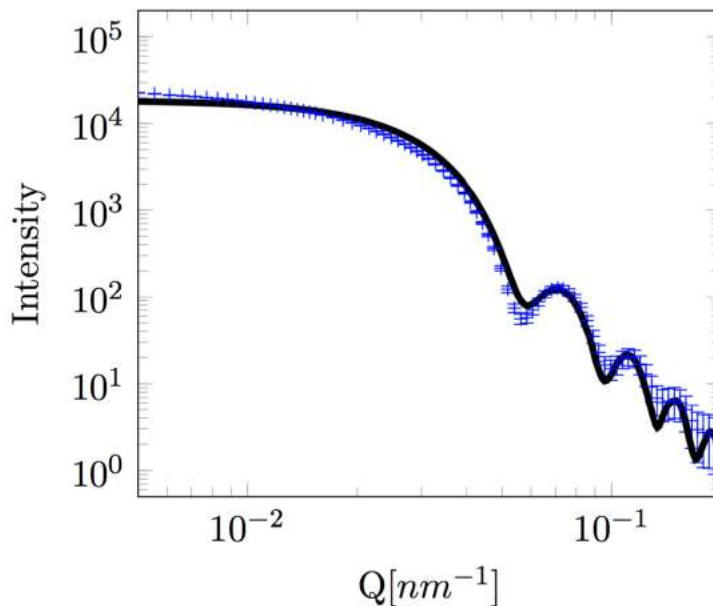


FIG. 3. USAXS measurement of the silica Stöber particles in H₂O, with a volume fraction of 0.01, measured on the beam line ID02 at the ESRF. The line is a fit to a hard-sphere model with radius of 83 ± 1 nm.

169 of as the scattering vector to the power -3.90 ± 0.03 , very close to the -4 expected from a
 170 perfectly smooth sharp particle surface.

171 DISCUSSION

172 Our model fits show clearly in figure 2 that the Stöber nano-particles can be well described
 173 as porous with both open and closed pores. The agreement between the particle radius
 174 derived from SESANS and USAXS is consistent, however both scattering methods return
 175 values significantly higher than that determined by our DLS measurements.

176 The inaccessible void structure is similar to that recently deduced from gas adsorption
 177 measurements by Li et al. [10]. The predicted value from SESANS of 10% inaccessible
 178 pores is close to that predicted by pycnometry of 13%. While in an earlier SESANS
 179 investigation [27] no porosity changes were observed and the SLD used for the particles was
 180 in good agreement with that obtained with bulk measurements. However in this case the
 181 silica particles were also covered by a sterically stabilizing layer of polyisobutene, 4 ± 5 nm
 182 thick. This disagreement with our results could be due to differences in the method used

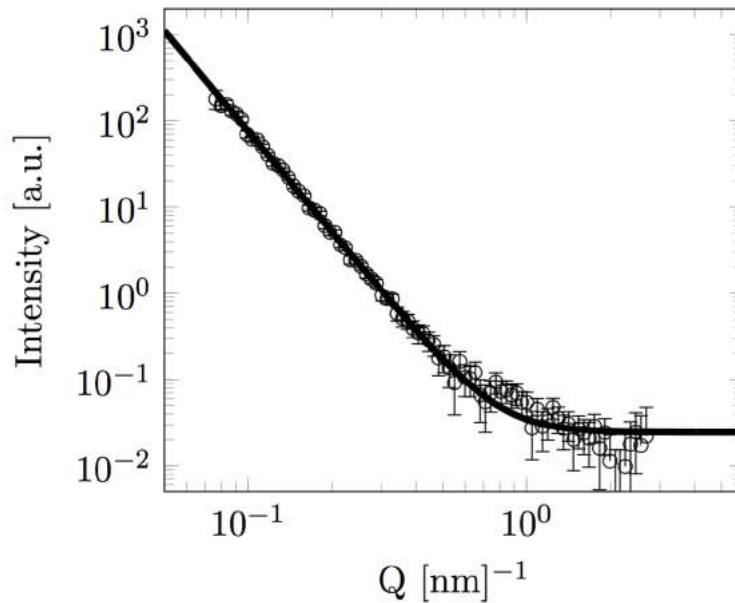


FIG. 4. SANS data for a low concentration solution of Stöber silica particles in D₂O. Line is fit to Porod scattering with a fractal index (n) of 3.90 ± 0.03 .

183 for particle formation or the hydrophobic coating blocking the pores and resulting in only
 184 closed pores, which appears more likely.

185 We observed scattering from smooth surfaces, which is consistent with earlier electron
 186 microscopy [14] and measured fractal indexes of Stöber particles with a long reaction time
 187 [7], unlike fractal surface previously observed by others [11, 28], albeit for larger particles.

188 CONCLUSIONS

189 The work shown in this communication, highlights the applicability of the SESANS tech-
 190 nique to both the study of colloids in solution and also porous media. The relatively trivial
 191 model used here allows for the extraction of both the inaccessible and accessible void volume
 192 fractions. The advantages of this technique arise from the unambiguous determination of
 193 the total scattering as given by the normalised spin-echo signal which is obtained at long
 194 spin-echo lengths. Also due to the insensitivity of the technique to incoherent scattering a
 195 series of samples can be prepared in H₂O and D₂O from the same master sample allowing the
 196 volume fractions to be determined as a ratio from one data set to another. This approach
 197 avoids the problem of separately determining the volume fraction and the contrast which

198 often plagues conventional SANS.

199 The technique can also be applied to larger Stöber particles and also to look at changes in
200 internal pore sizes where calcination is used to seal surface pores, however the consequence
201 of this upon the internal pore structure has yet to be investigated [29].

202 We have also shown that SESANS can easily be used to work with hydrogenous sam-
203 ples without the additional complications of incoherent scattering, unlike traditional SANS
204 experiments. Furthermore by analysis of the asymptotic value for the polarisation at long
205 spin echo length we are able to easily interpret the results without complex calibration and
206 corrections as would be required for the analysis using traditional small angle and ultra
207 small angle techniques.

208 APPENDIX A - SPIN-ECHO SMALL ANGLE NEUTRON SCATTERING

209 The SESANS theory has now been described in a number of publications [18, 30]. We
210 briefly summarise the salient points. The accessible spin-echo length for a neutron of wave-
211 length λ for our setup utilising a series of magnetic field is given by ;

$$z = cBL\lambda^2 \cot\theta \quad (1)$$

212 where c is a constant, L is the separation between the prisms and θ is the inclination angle of
213 the magnetic field boundary and the beam axis as defined in ref [31]. Therefore in any time
214 of flight experiment in which multiple wavelengths are used, a range of spin echo lengths are
215 probed simultaneously. In time of flight measurements the extent of this range is usually
216 chosen by selecting a particular static magnetic field strength (B).

217 The SESANS method encodes the scattering angle in the polarisation of the neutron
218 beam and the resulting change in polarisation from the scattering ($P(z)$) is given by;

$$P(z) = \exp(\Sigma_t[G(z) - 1]) \quad (2)$$

219 where Σ_t is the fraction of neutrons that are scattered once by a sample of thickness t and
220 $G(z)$ is a correlation function, related to the Debye-type correlation function, $\gamma(r)$ given
221 by [30];

$$G(z) = \frac{2}{\xi} \int_z^\infty \frac{\gamma(r)r}{(r^2 - z^2)^{\frac{1}{2}}} dr \quad (3)$$

222 where ξ is a normalising constant, given by;

$$\xi = 2 \int_0^\infty \gamma(r) dr \quad (4)$$

223 For a sample which scatters isotropically $G(z)$ is related to the neutron scattering cross
 224 section per unit volume of sample ($d\sigma/d\Omega$), as measured in a conventional SANS experiment
 225 by [30];

$$G(z) = \frac{\lambda^2 t}{2\pi \Sigma_t} \int_0^\infty J_0(qz) \frac{d\sigma}{d\Omega}(q) q dq \quad (5)$$

226 where $J_0(x)$ is the zeroth order cylindrical Bessel function. For homogeneous particles of
 227 SLD ρ the scattering cross section is related to the quantity $I(q)$ defined by Andersson et
 228 al. [30] as;

$$\frac{d\sigma}{d\Omega}(q) = \langle \Delta\rho^2 \rangle I(q) \quad (6)$$

229 here $\langle \Delta\rho^2 \rangle$ is the average of the squared scattering contrast as defined by Feigin and Svergun
 230 [32] for a system with either two or three scattering components as;

$$\langle \Delta\rho^2 \rangle = \sum_{i \neq j} \phi_i \phi_j (\rho_i - \rho_j)^2 \quad (7)$$

231 where ϕ_i and ρ_i are respectively the volume fraction and SLD of the i 'th component. Also
 232 using the more conventional SANS notation the scattering cross section is written as;

$$\frac{d\sigma}{d\Omega}(q) = \frac{N}{V} \langle \rho - \rho_0 \rangle^2 S(q) |F(q)|^2 \quad (8)$$

233 where $\frac{N}{V}$ is the particle number density and $S(q)$ and $F(q)$ are the structure and form factors
 234 respectively We use the equations for hard spheres, these are reproduced for clarity from
 235 reference [26] as suggested by the referees. Which for a hard sphere system $S(q)$ is calculated
 236 with the Percus-Yevick closure relation.

$$F(q, R) = \frac{[\sin(qR) - qR \cos(qR)]}{(qR)^3} \quad (9)$$

$$S(q) = \frac{1}{1 + 24\phi G(Rq)/(Rq)} \quad (10)$$

In this equation;

$$\begin{aligned} G(A) = & \alpha(\sin A - A \cos A)/A^2 \\ & + \beta(2A \sin A + (2 - A^2) \cos A - 2/A^3) \\ & + \gamma[-a^4 \cos A + 4((3A^2 - 6) \cos A + (A^3 - 6A) \sin A + 6)]/A^5 \end{aligned}$$

and

$$\begin{aligned}\alpha &= (1 + 2\phi)^2 / (1 - \phi)^4 \\ \beta &= -6\phi(1 + \phi/2)^2 / (1 - \phi)^2 \\ \gamma &= \phi\alpha/2\end{aligned}$$

237 where ϕ is the volume fraction of hard-spheres.

238 Finally the total (single) scattering probability (Σ_t) for a sample of thickness t is given
239 by;

$$\Sigma_t = \frac{\lambda^2 t}{2\pi} \int_0^\infty \frac{d\sigma}{d\Omega}(q) q dq = \lambda t \langle \Delta\rho^2 \rangle \xi \quad (11)$$

240 APPENDIX B- MODEL OF AN ISOTROPIC POROUS PARTICLE

241 In order to correctly model the silica Stöber particles we developed the following model,
242 which is valid for any homogeneous particle with open and closed pores. Assuming that
243 the volume fraction of accessible and inaccessible voids is V_{Open} and V_{Closed} respectively and
244 that the overall particle volume is V_P . The number of particles per unit volume of sample
245 is N we can write the mass fraction (MF) of the particles.

$$MF = \frac{NV_p(1 - V_{Open} - V_{Closed})d_p}{NV_p(1 - V_{Open} - V_{Closed})d_p + (1 - NV_p(1 - V_{Open}))d_L} \quad (12)$$

246 Where d_p is the mass density of the silica and d_l the mass density liquid. The term NV_p
247 is ϕ which is the volume fraction of the particles.

248 The density of the particles determined from the gas pycnometer measurements is given
249 by.

$$d = \frac{(1 - V_{Open} - V_{Closed})d_p}{(1 - V_{Open})} \quad (13)$$

250 The contrast difference defined in equation 7 can be written in terms of the scattering
251 length densities of the particle (ρ_p) and the liquid (ρ_l) given as;

$$\rho_p - \rho_l = (1 - V_{Open} - V_{Closed})\rho_S - (1 - V_{Open})\rho_l \quad (14)$$

252 Construction of LENS was supported by the National Science Foundation grants DMR-
253 0220560 and DMR-0320627, the 21st Century Science and Technology fund of Indiana,

254 Indiana University, and the Department of Defence. One of us, Steven Parnell acknowledges
255 funding from Oak Ridge National Laboratory. We thank the ISIS facility in the UK for the
256 award of beam time.

-
- 257 [1] B. Karmakar, G. De, and D. Ganguli, *Journal of Non-Crystalline Solids* **272**, 119 (2000).
258 [2] F. Vollmer, D. Braun, A. Libchaber, M. Khoshsima, I. Teraoka, and S. Arnold, *Applied*
259 *Physics Letters* **80**, 4057 (2002).
260 [3] I. M. White, N. M. Hanumegowda, and X. Fan, *Optics Letters* **30**, 3189 (2005).
261 [4] N. C. Bell, C. Minelli, J. Tompkins, M. M. Stevens, and A. G. Shard, *Langmuir* **28**, 10860
262 (2012).
263 [5] W. Stöber, A. Fink, and E. Bohn, *Journal of Colloid and Interface Science* **26**, 62 (1968).
264 [6] H. Boukari, J. Lin, and M. Harris, *Journal of Colloid and Interface Science* **194**, 311 (1997).
265 [7] H. Boukari, G. Long, and M. Harris, *Journal of Colloid and Interface Science* **229**, 129 (2000).
266 [8] D. Pontoni, T. Narayanan, and A. R. Rennie, *Langmuir* **18**, 56 (2002).
267 [9] G.H.Bogush, M.A.Tracy, and C.F.Zukoski-IVIV, *Journal of Non-Crystalline Solids* **104**, 95
268 (1988).
269 [10] S. Li, Q. Wan, Z. Qin, Y. Fu, and Y. Gu, *Langmuir*, *Langmuir* **31**, 824 (2014).
270 [11] V. M. Masalov, E. A. Kudrenko, N. A. Grigoryeva, K. V. Ezdakova, V. V. Roddatis, N. S.
271 Sukhinia, M. V. Arefev, A. A. Mistonov, S. V. Grigoriev, and G. A. Emelchenko, *Nano* **08**,
272 1350036 (2013).
273 [12] V. M. Masalov, N. S. Sukhinina, E. A. Kudrenko, and G. A. Emelchenko, *Nanotechnology*
274 **22**, 275718 (2011).
275 [13] C. A. P. Leite, E. F. d. Souza, and F. Galembeck, *Journal of the Brazilian Chemical Society*
276 **12**, 519 (2001).
277 [14] I. A. Karpov, É. N. Samarov, V. M. Masalov, S. I. Bozhko, and G. A. Emel'chenko, *Physics*
278 *of the Solid State* **47**, 347 (2005).
279 [15] R. Pynn, *Neutron Spin Echo*, edited by F. Mezei, *Lecture Notes in Physics*, Vol. 128, pp.
280 159–177. Heidelberg: Springer (1980).
281 [16] T. Keller, R. Gähler, H. Kunze, and R. Golub, *Neutron News* **6**, 16 (1995).
282 [17] M. T. Rekveldt, *Nuclear Instruments and Methods in Physics Research Section B: Beam*

- 283 Interactions with Materials and Atoms **114**, 366 (1996).
- 284 [18] A. L. Washington, X. Li, A. B. Schofield, K. Hong, M. R. Fitzsimmons, R. Dalgliesh, and
285 R. Pynn, *Soft Matter* **10**, 3016 (2014).
- 286 [19] C. Rehm, J. Barker, W. G. Bouwman, and R. Pynn, *Journal of Applied Crystallography* **46**,
287 354 (2013).
- 288 [20] M. T. Rekveldt, J. Plomp, W. G. Bouwman, W. H. Kraan, S. Grigoriev, and M. Blaauw,
289 *Review of Scientific Instruments* **76**, 033901 (2005).
- 290 [21] W. A. Hamilton, (2004), communicated by Wei-Ren Chen at NIST SANS Workshop.
- 291 [22] J. Plomp, V. O. de Haan, R. M. Dalgliesh, S. Langridge, and A. A. van Well, *Thin Solid*
292 *Films* **515**, 5732 (2007).
- 293 [23] C. M. Lavelle, D. V. Baxter, A. Bogdanov, V. P. Derenchuk, H. Kaiser, M. B. Leuschner,
294 M. A. Lone, W. Lozowski, H. Nann, B. v. Przewoski, N. Remmes, T. Rinckel, Y. Shin, W. M.
295 Snow, and P. E. Sokol, *Nuclear Instruments and Methods in Physics Research Section A:*
296 *Accelerators, Spectrometers, Detectors and Associated Equipment* **587**, 324 (2008).
- 297 [24] D. V. Baxter, J. M. Cameron, V. P. Derenchuk, C. M. Lavelle, M. B. Leuschner, M. A. Lone,
298 H. O. Meyer, T. Rinckel, and W. M. Snow, *Nuclear Instruments and Methods B* **241**, 209
299 (2005).
- 300 [25] S. R. Parnell, A. L. Washington, K. Li, H. Yan, P. Stonaha, F. Li, T. Wang, A. Walsh, W. C.
301 Chen, A. J. Parnell, J. P. A. Fairclough, D. V. Baxter, W. M. Snow, and R. Pynn, *Review*
302 *of Scientific Instruments* **86**, 023902 (2015).
- 303 [26] J. S. Pedersen, *Advances in Colloid and Interface Science* **70**, 171 (1997).
- 304 [27] T. Krouglov, W. G. Bouwman, J. Plomp, M. T. Rekveldt, G. J. Vroege, A. V. Petukhov, and
305 D. M. E. Thies-Weesie, *Journal of Applied Crystallography* **36**, 1417 (2003).
- 306 [28] M. Szekeres, J. Tóth, and I. Dékány, *Langmuir*, *Langmuir* **18**, 2678 (2002).
- 307 [29] N. Plumeré, A. Ruff, B. Speiser, V. Feldmann, and H. A. Mayer, *Journal of Colloid and*
308 *Interface Science* **368**, 208 (2012).
- 309 [30] R. Andersson, L. F. Van Heijkamp, I. M. De Schepper, and W. G. Bouwman, *Journal of*
310 *Applied Crystallography* **41**, 868 (2008).
- 311 [31] J. Plomp, V. de Haan, R. Dalgliesh, S. Langridge, and A. van Well, *Physica B: Condensed*
312 *Matter* **406**, 2354 (2011).
- 313 [32] L.A.Feigin and D.I.Svergum, *Structure Analysis by Small Angle X-ray and Neutron Scattering*

314 (Pelnum, New York, 1987).